reduction in intensity but shifted the maximum to a lower wavelength. Furthermore, the fluorescence intensity of the reduced solution was quite sensitive to optical path. Back fluorescence from the face of the cuvette was stronger than that measured with a 90° path through the cell. These observations together indicate that the fluorescence intensity observed is not directly proportional to concentration so that fluorescence quenching and/or inner filter effects are likely.

The shoulder for the absorption spectra of discharged electrolyte at 500 nm is close to the maximum in the wavelength excitation scan at 510 nm. It therefore appears, that a single species accounts for both features and for the strongly enhanced fluorescence at 550-600 nm.

Electron spin resonance studies in dimethylformamide show that at SO_2 concentrations above 0.05*M*, a single free radical species, $(SO_2)SO_2^-$, is produced during the controlled one-electron reduction of SO_2 (10). Using ultraviolet-visible spectroscopy, this free radical dimer has been associated with a strong absorption at 580 nm in this solvent (11). Furthermore, electrochemical studies have shown that this dimer is stable in acetonitrile and hexamethylphosphoramide (12), amide solvents (13), n-methylpyrrolidinone (14), and even metastable in water (15). It is, therefore, tempting to assign the absorption of 500 nm and resultant fluorescence in electroreduced $SOCl_2$ to $(SO_2)SO_2^-$ dimer. Electron spin resonance measurements of reduced $SOCl_2$ electrolyte support the existence of at least one free radical species stable in the $LiAlCl_4$-$SOCl_2$-SO_2 media (1, 2).

On the other hand, a strong Raman emission at 1081 cm^{-1} detected for $(SO_2)SO_2^-$ generated in DMF (13) is absent in Raman spectra of extensively discharged Li/$SOCl_2$ electrolyte, although it may account for the infrared absorption at 1070 cm^{-1} occurring in freshly discharged $SOCl_2$ (1).

Positive identification of the fluorescing species must await careful correlation of electron spin resonance, Raman, fluorescence, and voltammetry results in $SOCl_2$ and supporting solvents. Current efforts in this laboratory are focusing on the stability of the fluorescence and its dependence on exciting wavelengths and electrolyte salt.

The technique of fluorescence spectroscopy offers promise in the search for a more complete picture of the chemical and electrochemical reactions of $SOCl_2$. The complex optical interaction between absorption, excitation, and fluorescence in these solutions offers a challenge in arriving at a correct interpretation.

Acknowledgments

The author wishes to thank Mr. James Bennett and Mr. Richard Mank for help in preparing electrolytes, Mr. William McHugh for discharging cells, and Mr. Roger Hunt for help in collecting the excitation spectrum.

Manuscript submitted April 20, 1987; revised manuscript received Sept. 10, 1987.

GTE Government Systems Corporation, Strategic Systems Division, assisted in meeting the publication costs of this article.

REFERENCES

1. R. C. McDonald, F. W. Dampier, P. Wang, and J. M. Bennett, Final Report, Contract N60921-81-C-0229, November 1982.
2. B. Carter, R. Williams, A. Rodriquez, F. Tsay, and H. Frank, Paper 293 presented at The Electrochemical Society Meeting, Detroit, MI, Oct. 17-21, 1982.
3. W. Clark, F. W. Dampier, R. C. McDonald, A. Lombardi, D. Batson, and T. Cole, AFWL-TR-85-2003, December 1984.
4. M. C. Dhamelincourt, F. Wallart, P. Barbier, G. Mairesse, and P. Descroix, *J. Power Sources*, **14,** 77 (1985).
5. J. C. Touchstone, R. A. Keisman, A. F. Marcantonio, and J. W. Greene, *Anal. Chem.*, **30,** 1707 (1958).
6. S. Brownstein, E. Gabe, F. Lee, and L. Tan, *J. Chem. Soc.*, 1566 (1984).
7. D. Wong, W. Bowden, N. Hamilton, V. Cubbison, and A. N. Dey, DELET-TR-78-0583-F, Contract No. DAAB07-78-C-0563, April 1981.
8. K. French, P. Cukor, C. Persiani, and J. J. Auborn, *This Journal*, **121,** 1015 (1974).
9. F. M. Delnick and W. R. Cieslak, Paper 145 presented at The Electrochemical Society Meeting, New Orleans, LA, Oct. 7-12, 1984.
10. B. Kastening and B. Gostisa-Mihelcic, *J. Electroanal. Chem.*, **100,** 801 (1979).
11. R. P. Martin and D. T. Sawyer, *Inorg. Chem.*, **11,** 2644 (1972).
12. C. L. Gardner, D. T. Fouchard, and F. C. Laman, in "Power Sources for Biomedical Implantable Applications and Ambient Temperature Lithium Batteries," B. Owens and N. Margalit, Editors, p. 545, The Electrochemical Society Softbound Proceedings Series, Pennington, NJ (1980).
13. R. G. Rinker and S. Lynns, *J. Phys. Chem.*, **72,** 4706 (1968).
14. P. Anantaraman, P. Archaubault, R. Day, and C. Gardner, in "Lithium Batteries," A. N. Dey, Editor, p. 231, The Electrochemical Society Softbound Proceedings Series, Pennington, NJ (1984).
15. S. Lynn, R. G. Rinker, and W. H. Corcoran, *J. Phys. Chem.*, **68,** 2363 (1964).

A Technique for Delineation of PN Junctions in Cubic Silicon Carbide

G. L. Harris and K. Fekade

Electrical Engineering Department, Solid State Electronic Group, Howard University, Washington, D.C. 20059

Recently, cubic silicon carbide has been receiving a tremendous amount of attention in the semiconductor world (1-3). Its large bandgap, high saturation velocity, radiation hardness, and relatively large low field mobility are just a few of its properties which make it a candidate for high temperature radiation resistant semiconductor devices. Kondo and co-workers (4) have reported on SiC MESFET devices. If continued improvements are to be made on these and other devices, it must be possible to control and measure junction depth to within a few hundred angstroms. In this technical note, we briefly describe a highly precise technique for delineating pn junctions in beta SiC grown on silicon substrates.

Experimental Discussion

The epitaxial SiC layers used for the development of this technique were grown at 200 torr by reacting propane (C_3H_8) and silane (SiH_4). The growth temperature was approximately 1343°C and a carbonized layer of SiC was used to reduce the strain at the interface between the SiC and silicon. A complete description of this process and the CVD system is provided by Harris (5). The p-type dopant

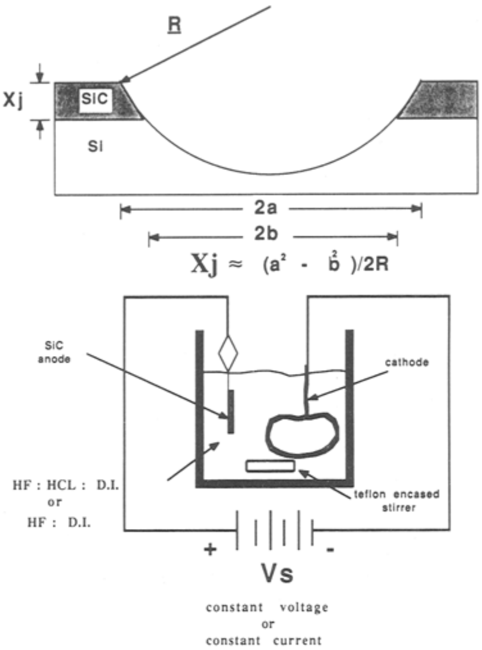

Fig. 1. Junction sectioning technique and anodic oxidation procedure. (a, above) Cross-sectional diagram of a sectioned junction. (b, below) Anodic oxidation apparatus.

Table I. A summary of n layer thicknesses measured by the junction sectioning and selective anodizating technique

pn junction delineation summary

n layer growth time (min)	n layer thickness (μm)	Total thickness (2h growth) (μm)
10	0.457	5.93
14	0.598	6.13
20	0.916	6.12
60	2.15	6.68

was Al which was obtained by bubbling H_2 through trimethylaluminum in a stainless steel vessel placed in a temperature bath at 17.4°C. The undoped layers were-type and the structures were np (SiC) on (100) p-type silicon substrates with $r > 120$ V-cm. The growth rate of the SiC was approximately 3.0 μm/h with a Si/C ratio equal to one in the gas phase.

To determine the junction depth, a cylindrical groove was ground into the np junction until the silicon was reached. The grooving was performed using a Philtec Model 2105 sectioning system employing a diamond paste (DWD-06). This visually magnified the SiC/Si junction and the total thickness of the SiC layer could easily be determined without any selective etching because of the differences in the indexes of refraction. If R is the radius of the grooving cylinder and a and b are as indicated in Fig. 1a, then for $R >> a$ and b

$$X_j \approx a^2 - b^2/2R$$

where X_j is the junction thickness.

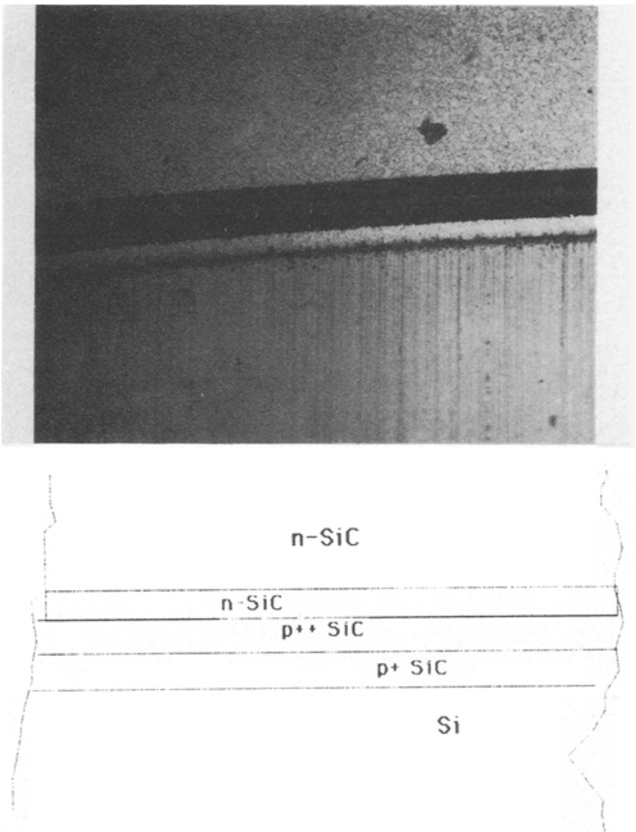

Fig. 2. Nomarski micrograph of a n-SiC/p^{++}-SiC/p-SiC/p-Si junction which has been selectively anodized.

The selective etching of the SiC was carried out by placing the grooved semiconductor in an electrolytic cell. Using stainless steel tweezers, the positive terminal of the power supply was connected to the SiC which served as the anode. A stainless steel loop of tubing connected to the negative terminal of the supply served as the cathode and both were placed in a Teflon beaker with the electrolyte (see Fig. 1b). The source impedance of the supply was very low; therefore, the selective etching took place under constant voltage conditions. HF:DI water (1:50) served as the electrolyte. The HF acid also was an electrolytic etchant. In this case, the oxide dissolved as rapidly as it formed and no oxide stripping rinse was required for this anodization process.

During the anodization process, a source of surface ions from the n and p regions of the SiC are required to combine with $(OH)^-$ to form a hydroxide (6). The n-type layer is biased positive and the oxide-semiconductor interface behaves as a reverse biased Schottky contact (7). Current in this region results from avalanche breakdown. In the p-type region, the oxide-semiconductor diode is forward biased producing its source of ions. As the layer of SiC is consumed during the growth of the oxide, the etching rate of the n and p regions are governed by the currents through their respective cross-sectional regions. This variation in current results in a junction delineation.

Results and Conclusions

Shown in Fig. 2 is one side of a grooved and anodized np junction of SiC/Si. During selective etching which lasted approximately 10s, the source anode voltage was 30V and the sample current was 0.1 mA. This time interval produced homogeneous and reproducible data for the range of samples investigated. The demarcation lines on the micrograph represent the n-SiC/p^{++}-SiC, the p^{++}-SiC/p-SiC, and the p-SiC/Si interfaces, respectively, from top to bottom. Near the p-SiC/Si interface the boundary appears darker because of the rounding effect of the sectioning machine. The magnification of this micrograph was approximately 104 times and the n layer thickness was 2.15 μm with a total thickness of 6.63 μm. The p layer was grown for 2h and the n layer for 60 min at 1343°C. The variation across a 1 1/2 in. piece of SiC was approximately 30% for the two thicknesses. Table I is a summary of the n layer thickness measured at various growth times using the developed delineation technique. This grooving and anodization technique appears to be very useful in determining junction thicknesses in beta SiC and may also be useful in other polytypes of SiC.

Acknowledgments

Special acknowledgment is made to NASA-Lewis (NAG-3-431) and Howard University (AA61A) for their much needed and appreciated support.

Manuscript submitted Oct. 16, 1986; revised manuscript received July 31, 1987.

Howard University assisted in meeting the publication costs of this article.

REFERENCES

1. S. Yoshida, K. Saaki, E. Sakuma, S. Misawa, and S. Gonda, *Appl. Phys. Lett.*, **46,** 766 (1985).
2. J. Ryu, H. J. Kim, and R. F. Davis, *ibid.*, **47,** 850 (1985).
3. S. Dohmae, K. Shibahara, S. Nishino, and H. Matsunami, *Jpn. J. Appl. Phys.*, **24** (11), 835 (1985).
4. Y. Kondo, T. Takahashi, K. Ishii, Y. Hayashi, E. Sakuma, S. Misawa, H. Daimon, M. Yamanaka, and S. Yoshida, *IEEE Electron Device Lett.*, **EDL-7,** 404 (1986).
5. G. L. Harris, K. H. Jackson, G. J. Felton, K. R. Osborne, K. Fekade, and M. G. Spencer, *Mater. Lett.*, **4** (2), 404 (1986).
6. S. K. Ghandhi, "VLSI Fabrication Principles," Chap. 7, J. Wiley & Sons, Inc., New York (1982).
7. D. L. Rode, B. Schwartz, and J. V. DiLorenzo, *Solid-State Electron.*, **17,** 1119 (1974).

ERRATA

In the paper titled "Aqueous Redox Transition Model Complexes for Electrochemical Applications as a Function of pH," by J. G. Ibanez, C.-S. Choi, and R. S. Becker (to whom correspondence should be addressed) *This Journal,* **134,** 3083 (1987), the captions for Fig. 2 and Fig. 3 were reversed. The correct captions and figures are below.

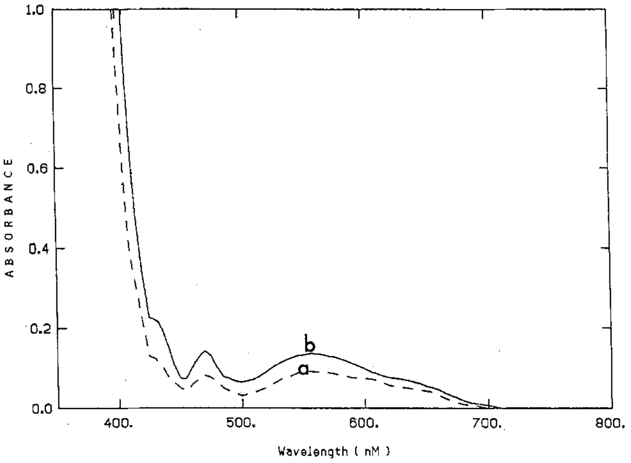

Fig. 2. Absorption spectra: (a) for 0.15*M* Fe(III)-TEA complex containing 3*M* NaOH, 0.4*M* KCl, *p*H 13; (b) for 0.15*M* Fe(III)-TEA and 0.15*M* Fe(II)-TEA mixture containing 3*M* NaOH, 0.4*M* KCl, *p*H 13. The wavelength was scanned from 800 to 400 nm. A quartz cell with pathlength of 5 mm was used.

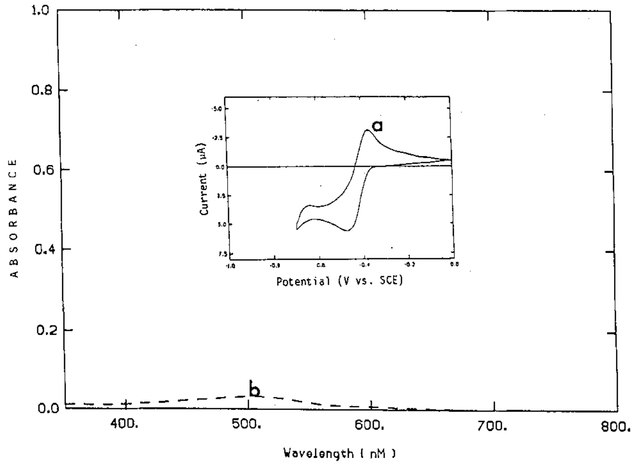

Fig. 3. Cyclic voltammetric curve and absorption spectrum of the solution of 5 mM $[Co(II)EN_3]^{2+}$, 0.1*M* KCl, and *p*H 2.7: (a) Cyclic voltammetric curve at the Pt electrode. (The potential was multiply scanned between 0.0 and −0.7V with a scan rate 50 mV/s) (the third scan is shown); (b) absorption spectrum of the same solution as cyclic voltammetric experiment. (The wavelength was scanned from 800 to 350 nm. A Pyrex cell with pathlength of 10 mm was used).

In the paper titled "Modeling of LPCVD reactors. Effect of Empty Inlet Tube," by M. G. Joshi *This Journal,* **134,** 3118 (1987) Eq. [1] and [3] should read

$$\mathfrak{R} = \frac{k p_{SiH_4}}{1 + K_H p_{H_2}^{1/2} + K_S p_{SiH_4}} \left(\frac{mol}{m^2 \cdot s}\right) \qquad [1]$$

$$\frac{1}{\xi}\frac{d}{d\xi}\left(\frac{\xi}{1 + \epsilon\chi}\frac{d\chi}{d\xi}\right) + \Phi^2 g[\chi(\xi)] = 0 \qquad [3]$$